

THE CLOSEST VIEW OF A DWARF GALAXY: NEW EVIDENCE ON THE NATURE OF THE CANIS MAJORIS DWARF SATELLITE

DAVID MARTÍNEZ-DELGADO, DAVID J. BUTLER, HANS-WALTER RIX, Y. ISABEL FRANCO AND JORGE PEÑARRUBIA
 Max-Planck Institut für Astronomie, Königstuhl, 17 D-69117 Heidelberg, Germany

Draft version February 7, 2020

ABSTRACT

We present a first deep colour-magnitude diagram of the central region ($0.5^\circ \times 0.5^\circ$) of the Canis Majoris stellar over-density ($(l, b) = (240, -8)$) found by Martin et al. (2004) that has been proposed as the remnant of a dwarf satellite accreted onto the Milky Way on a near-equatorial orbit. We find a narrow, main-sequence extending 6 magnitudes below the cut-off to our limiting magnitude ($B \sim 24.5$ mag). This main sequence has very high contrast with respect to the thin/thick disk/halo background; its narrowness at brighter magnitudes clearly implies the presence of a distinct and possibly still bound stellar system.

We derived the line-of-sight size ($r_{1/2}$) of this system based on the B-band width of the lower main sequence, obtaining 0.93 ± 0.25 (random) ± 0.36 (systematic) kpc. That size matches a model prediction for the main body of the parent galaxy of the Monoceros tidal stream, and rejects the alternative explanation of a flared or warped Galactic disk viewed in projection (Monamy et al. 2004). We also derived a central surface brightness of $\mu_{V,0} \geq 24.1 \pm 1.8$ mag arcsec $^{-2}$ and an absolute magnitude of $M_V = -13.8 \pm 1.8$ mag. These values place the Canis Majoris object in the category of dwarf galaxy in the L_V -size and $M_V - \mu_V$ planes for such objects. However, like the Sagittarius dwarf, it is an outlier in the $[\text{Fe}/\text{H}] - M_V$ plane in the sense that it is too metal rich for its estimated absolute magnitude. This suggests that the main mechanism driving its recent and current star formation history (possibly tidal stripping) is different to that of isolated dwarfs.

Subject headings: galaxies: dwarf — galaxies: fundamental parameters — galaxies: individual (Canis Majoris) — galaxies: spheroidal — galaxies: stellar content — galaxies: structure

1. INTRODUCTION

The Milky Way offers a unique laboratory for testing the hierarchical galaxy formation scenario through the study of past distinct merger events, which may take the form of long stellar streams or large scale substructures in the Galactic halo or even in the disk (Navarro 2004, and references therein). The resolution of such tidal streams into stars and the measurement of phase-space coordinates for these stars allows one to gather the fossil records of their evolution with unparalleled accuracy. These can be directly compared with N-body simulations in order to reconstruct their dynamical history and their impact on the Milky Way at the present and recent epochs.

Recently, the Sloan Digitized Sky Survey (SDSS) team reported the discovery of a coherent giant stellar structure at low galactic latitudes (Newberg et al. 2002; Yanny et al. 2003), which appears to form a ring around the Milky Way. Since then, there has been a tremendous amount of follow-up observational effort probing its structure and kinematics in order to understand its origin (see Majewski 2004 and references therein). N-body simulations (Martin et al. 2004a; Peñarrubia et al. 2004) shows that this ring structure can be naturally attributed to the tidal stream of a dwarf galaxy (named the Monoceros tidal stream, or the Galactic Anticenter tidal stream). The position of the main body of its parent galaxy is still controversial. The best candidate is the Canis Majoris (CMa) dwarf galaxy candidate, a strong ellipse-shaped over-density of red giant stars discovered in this constellation by Martin et al. (2004a) from an analysis of the 2MASS survey. Bellazzini et al. (2004)

presented a color-magnitude diagram (CMD) in the surroundings of the candidate CMa dwarf, concluding that the system is situated at 8 ± 1 kpc from the Sun and that it is composed of a metal-rich, intermediate-age stellar population. As an alternative interpretation, Momany et al. (2004) suggested that this over-density is the signature of the Galactic warp in this direction of the sky. In response to this criticism, Martin et al. (2004b) reported a narrow radial velocity distribution for the center of this structure, consistent with the hypothesis of an accreted dwarf satellite in the Galactic plane.

In this paper, we present deep broad-band photometry of the CMa center with the aim of shedding light on the controversial nature (dwarf galaxy or Galactic perturbation) of this stellar system. As our results confirm and greatly strengthen the case that the stellar over-density towards CMa is a distinct dwarf galaxy, we refer to it as 'CMa dwarf' throughout.

2. OBSERVATIONS AND DATA REDUCTION

Our observations were carried out in B and R Johnson-Cousins filters with the 2.2m ESO/MPG telescope at the La Silla Observatory (Chile) in service mode during December 14-17th, 2003. We used the Wide-Field Imager (WFI) installed at the prime focus, which holds eight 2046×4098 pixel EEV chips, with a scale of $0.238''$ pixel $^{-1}$. Our field covers a total area of about 0.25 deg 2 and is centered at galactic coordinates $(l, b) = (240.15, -8.07)$, which is, within the uncertainties, the nominal center of the CMa over-density given by Martin et al. (2004a). The total exposure times were 3700s and 2700s in B and R respectively. A shorter exposure of 100s in

both bands was also taken to recover the brighter part of the CMD.

Bias and flat-field corrections were done with IRAF. DAOPHOT and ALLSTAR (Stetson 1994) were used to obtain the photometry of the resolved stars. Aperture corrections were estimated using a set of about 50 isolated, bright stars in the CMa frame, with a variance of $\sigma \sim 0.001$. Transformation of the instrumental magnitudes into the standard photometric system were obtained from observations of the Landolt standard field SA95 taking during several photometric nights bracketing our observations and using the atmospheric extinction coefficients estimated on November 8th, 2003 taken from the WFI homepage. Putting all the errors together, the total zero-point error of our photometry can be estimated to be about $\sigma = 0.02$ for all bands. The resulting catalogue of stars was filtered using the error parameters given by ALLSTAR, retaining only stars with acceptable CHI and SHARP parameters and $\sigma_B < 0.2$ and $\sigma_R < 0.2$.

Artificial star tests were performed in the usual way (see Aparicio, Carrera & Martínez-Delgado 2001) using a total of 20000 artificial star to check the observational effects and estimate the completeness factor as a function of magnitude.

3. THE COLOR-MAGNITUDE DIAGRAM

Fig. 1a shows the $[B - R, R]$ CMD of the center of the possible CMa dwarf based our $t_{exp} = 100s$ data. The stellar densities in this CMD confirm immediately that the distribution of stars in the Milky Way in this low-latitude direction grossly deviate from the expectations of a smooth thin/thick/halo distribution: there is a conspicuous main-sequence (MS) feature, with a possible arc-shape turnoff at $R \sim 17.8$ (see Sec. 4.1). The $B - R$ colour used on our CMD provides a better separation of the red plume populated by red giants of the Galactic warp from this MS feature, which is about ~ 0.2 mag bluer at $R \sim 18$ (see also Bellazzini et al. 2004). Secondly, a second plume of possible blue stragglers (labelled *BS* in Fig. 1a) is observed extending brighter and bluer than the MS-turnoff and reaching $R \simeq 16.0$, avoiding the Galactic star contamination¹. This blue extension is similar to those observed in the CMD of Local Group (LG) dwarf spheroidal (dSph) galaxies (Draco:Aparicio et al. 2001; Ursa Minor: Carrera et al. 2003) and cannot be reproduced by any star-count models of the Milky Way (see also Bellazzini et al. 2004). The narrow distribution of these blue stars strongly suggests that they are all at a similar distance, which would not be expected if the Galactic warp/flare were the origin of this stellar population. Our diagram also shows evidence of a possible red clump (labelled *RC* in Fig. 1a) at $(B - R) \sim 1.5$ and $R \sim 16.5$, but a suitable control field or radial velocity follow-up is necessary to confirm this over-density as part of the CMa dwarf.

Fig. 1b shows the $[B - R, B]$ CMD based on our long exposure data. This CMD reveals a prominent, high contrast, and well-populated MS feature extending beyond our limiting magnitude ($B \sim 24.5$). The colour width of this MS feature remains roughly constant along a large

¹ This blue sequence could be produced by MS stars rather than by blue stragglers, suggesting that the CMa system has had at least two distinct epochs of star formation

magnitude range and is comparable to those observed in the CMD of Local Group dwarf galaxies or massive globular clusters. This evidence strongly confirms the presence of a limited range in distance, and therefore associated with a possibly still bound stellar system whose distance line-of-sight size and stellar density are investigated in the next section.

4. PROPERTIES OF THE CANIS MAJORIS DWARF GALAXY

4.1. Distance

Our CMD does not show any unambiguous convincing signature of the bright populations² (red clump, horizontal branch, RR Lyrae stars, red giant branch stars) extensively used to constrain the distance and stellar population properties of LG dwarf galaxies. However the distance to CMa dwarf can be obtained from the apparent R-band magnitude of the MS turn-off, assuming that the stellar population of the galaxy is known. This last value and its uncertainty was estimated using a bootstrap approach (see Butler, Martínez-Delgado & Branner 2004) from the long exposure CMD (Fig.1b). We adopt $E(B-V) = 0.213 \pm 0.029$ mag for our field from the Schlegel, Finkbeiner & Davis (1998; SFD98) dust map. This yields an apparent (dereddened) R-band magnitude for the MS-turnoff of $m_{MS,r,0} = 17.88 \pm 0.10$. Assuming that we adopt the absolute MS turn-off magnitude of an old population (15 Gyr, with $Z=0.006$), for which we measure $M_{MS,R} = +3.840 \pm 0.004$, one obtains an upper limit on the distance modulus of $(m - M)_o = 14.5 \pm 0.1$ ($d_\odot = 8.1 \pm 0.4$ kpc). For the younger stellar population reported by Bellazzini et al. (2004), one gets $M_{MS,R,0} = +4.740 \pm 0.004$, and $(m - M)_o = 13.6 \pm 0.1$ ($d_\odot = 5.3 \pm 0.2$ kpc). This distance range is compatible with previous estimates based on different CMD indicators (Bellazzini et al. 2004; Martin et al. 2004b).

4.2. Line-of-sight size of the CMa dwarf galaxy

Monamy et al. (2004) proposed that the Galactic warp and flare models of the disk can explain the stellar density and morphology of shallow CMDs of the CMa over-density. However, our deeper data shows a conspicuous narrow MS feature in the CMD (Sec. 3) that clearly suggests that the CMa over-density is a distinct entity and not a projection effect of the thin disk in presence of the proposed Milky Way perturbations.

To derive the line-of-sight size of CMa, our approach has been to derive the associated photometry spread, ΔB in the observed MS. Firstly, we obtained the B-band distribution of star counts in the $(B - R)$ range 1.50-1.55 mag using the long exposure data (see Fig. 1b). We then modelled this distribution as the linear sum of two components, namely a smooth tilted distribution of underlying stars due to the Galactic warp and thin disk, and the CMa MS. The B-band shape of the MS is modelled as a gaussian function, characterized by a standard

² The near-absence of these two features in the CMD is consistent with our preliminary model CMDs of the CMa dwarf (Martínez-Delgado et al., in preparation), which shows that, for its possible metal-rich stellar population (see Bellazzini et al. 2004), the corresponding RGB is very dispersed in colour and poorly populated, which is what gives it a very low contrast against the Galactic disk stars. The obvious MS observed here has no significant impact on that explanation.

deviation σ_{MS} . σ_{MS}^2 is taken as the sum, in quadrature, of three components: the intrinsic MS size,³ $\sigma_{\text{MS int}}$; the contribution to the MS width from observational effects, estimated from artificial star trial (see Sec.2); and the differential reddening of the field, estimated from the SFD98 dust maps. In brief, we fitted the distribution in Fig. 2 (in a χ^2 sense) to a linear function at $B=20$ -20.5 and 23.5-24 mag and fitted a gaussian function in non-linear least squares way after subtracting the linear fit. The fitting was repeated for two adjacent colour intervals in order to obtain a statistical uncertainty in the MS width. Their mean and standard deviation data is given in Table 1, together with the rest of the budget used to determine the line-of-sight size of CMa (i.e., ΔB).

Our best fitting ΔB (taken as $\pm 1\sigma$), converted into kilo-parsecs, yields $1.60 \pm 0.20 \pm 0.10 \text{ kpc}$ or $\text{FWHM} = 1.92 \text{ kpc}$ (see Table 1). Based on 2MASS data, Martin *et al.* (2004b) report that angular extent of the system corresponds to a FWHM of about $\sim 4.2 \text{ kpc}$ (at a heliocentric distance of $7.1 \pm 1.3 \text{ kpc}$), significantly larger than the line-of-sight value estimated here. This is not necessarily inconsistent, because severe tidal perturbations may cause a tangential stretching of the CMa dwarf. In addition, the estimated size of CMa dwarf can provide a reliable estimation of its mass under the assumption that bound stellar systems undergoing disruption have a spatial extension similar or larger than the Jacobi limit, as Peñarrubia *et al* (2004) find for the Monoceros stream progenitor. In that case (Binney & Tremaine 1986; equation 7-84),

$$M_s \sim 3M(< R_{\text{gal}})(R_t/R_{\text{gal}})^3$$

where $M(< R_{\text{gal}})$ is the Galaxy mass within R_{gal} and R_t is the Jacobi limit (also called tidal radius). Adopting $R_t \simeq 1.6$ (which accounts approximately for 96% of the dwarf mass) and the mass profile used by Peñarrubia *et al.* (2004) we find $M_s > 5 \times 10^8 M_{\odot}$, indicating that the present mass of the CMa dwarf should be similar to those predicted by our model of the Monoceros stream progenitor ($3 \times 10^8 M_{\odot}$: Peñarrubia *et al.* 2004).

Finally, in order to compare the size of CMa with those of known dwarf galaxies, we estimate the line-of-sight half-brightness radius, $r_{1/2}$, from the gaussian model of the line-of-sight profile given in Fig. ???. We obtain $r_{1/2}=0.93 \pm 0.25$ (random) ± 0.36 (systematic) kpc, in agreement with the model prediction (Peñarrubia *et al.* 2004); but is significantly bigger than that of several dwarf galaxies in the LG (Irwin & Hatzidimitriou 1995; their Table 4).

4.3. Surface brightness and total luminosity

We estimate the central surface brightness (SB) of the CMa dwarf by matching the observed surface density of MS stars to scale those derived in two different CMDs for which the integrated magnitude is known: i) the synthetic CMD for the CMa galaxy (2.5-15 Gyr; $Z=0.006$) and ii) the CMD of the center of the Sagittarius (Sgr) dSph from Martínez-Delgado *et al.* (2004). For case (i) we used the short exposure data and counted stars on the upper MS in a small box such that $0.25 < B - R < 0.6$

³ This was obtained from a synthetic CMD computed for a constant and arbitrary star formation rate between 4 and 10 Gyr and $Z = 0.006$ ($[\text{Fe}/\text{H}] = -0.48 \text{ dex}$).

and $16 < R < 17.5$; the position of this CMD box avoids significant contamination from the red plume of Galactic disk stars⁴. We find $\mu_{V,0} = 25.4 \pm 0.5 \text{ mag arcsec}^{-2}$ (taken as the intensity-weighted average of $\mu_{B,0}$ and $\mu_{R,0}$), where the SB uncertainty was estimated by taking Poisson statistical errors in the star counts. For our second SB estimate, based on the comparison with a Sgr CMD, we counted stars at $1.0 < B - R < 1.1$ and $18.2 < R < 18.4$ in our CMa CMD, and at the corresponding location in the Sgr CMD (i.e. accounting for extinction and distance differences, and assuming similar stellar population for both systems). As contamination by Galactic stars may have been under-estimated, we obtain $\mu_{R,0} \geq 22.8 \pm 0.4 \text{ mag arcsec}^{-2}$. The mean of both estimates is $\mu_{B,0} \geq 24.1 \pm 1.8 \text{ mag arcsec}^{-2}$, which we take as our best value for the central SB of the CMa dwarf. That value is very similar to those of Milky dSph satellites (Mateo 1998), and is additional evidence that we have detected the main body of a dwarf galaxy and not a piece of a possible tidal stream, whose typical SB would be expected to lie in the range of 30.0 to 31.5 mag arcsec^{-2} (Johnston *et al.* 1999).

To estimate the total V-band luminosity, we use an exponential SB profile with a (near-IR) scale height of $0.73 \pm 0.05 \text{ kpc}$ (Martin *et al.* 2004a) with the mean heliocentric distance taken to be 7.1 kpc. We obtained $M_V = -13.8 \pm 1.8 \text{ mag}$, corresponding to a total V-band intensity log $(I_V/I_{V,\odot}) = 7.4 \pm 0.7$. This yields a total mass for the satellite of $M/M_{\odot} = 2.5 \times 10^7 \Gamma$ (where $\Gamma = M/M_{\odot}/L/L_{\odot}$). Assuming the mass-to-light ratio of CMa is in the range $4 < (M/L) < 22$, in solar units, (which contains the majority of the LG dSphs), the present remnant of the CMa dwarf would have a total mass of $1.0 < \Gamma < 5.5 \times 10^8$, consistent with the value obtained from the observational extension of the satellite and from the prediction of our theoretical simulations (see Sec. 4.2). The combination of this luminosity with the size derived in Sec. 4 places this stellar system among the dwarf galaxies in the the L_V -size plane (see Pasquali *et al.* 2004; their Fig. 5). In addition, CMa follows the well-defined $M_V - \mu_V$ relationship shown by Caldwell *et al.* (1999) for dwarf galaxies. However, assuming the stellar component of the galaxy has an average metallicity of $[\text{Fe}/\text{H}] \sim -0.4$ (Bellazzini *et al.* 2004), this galaxy is, like the Sgr dSph, an outlier of the well-known $[\text{Fe}/\text{H}] - M_V$ relation, since it is too metal rich for its estimated absolute magnitude. This suggests, as in the case of Sgr, that a different mechanism (possibly tidal stripping) is predominantly driving its star formation history.

Derived parameters for the CMa system are given in Table 2.

5. DISCUSSION

The line-of-sight size derived from our deep CMD of the center of CMa over-density strongly supports the interpretation of a distinct, possibly still bound stellar system whose properties are consistent with those expected for the remnant of a partially disrupted dwarf satellite.

⁴ Because of the lack of a suitable control field to correct the MS star-counts for contamination from Milky Way stars, we use instead a synthetic CMD of the Galactic field in this direction computed from the Galactic model through a www interface (Robin *et al.* 2003)

The high density contrast and limited line-of-sight extent of the CMa feature rule out a flared or warped Galactic disk viewed in projection (Momamy et al. 2004). Although the obtained properties for this satellite (Table 2) in this study are subject to considerable uncertainties (stellar population, Galactic contamination, radial profile), they are in agreement with those of the known Milky Way dSph satellites (Mateo 1998) and with the known size-luminosity relation followed by Milky Way dwarf spheroidals.

At a distance of 8 kpc, CMa is the closest dwarf galaxy known. It may not only be the parent of the Galactic low-latitude stellar stream, but also a unique laboratory for testing galaxy evolution theories. In particular, our CMD shows the availability for first time of thousands of MS stars of different ages in a magnitude range suited to high resolution spectroscopy-based abundance studies using 4-meter class telescopes. This will allow one to study the SFH of a dwarf galaxy with unprecedented spectral resolution, and is therefore a top candidate for chemo-dynamical modelling of dwarf galaxy evolution in the Galaxy.

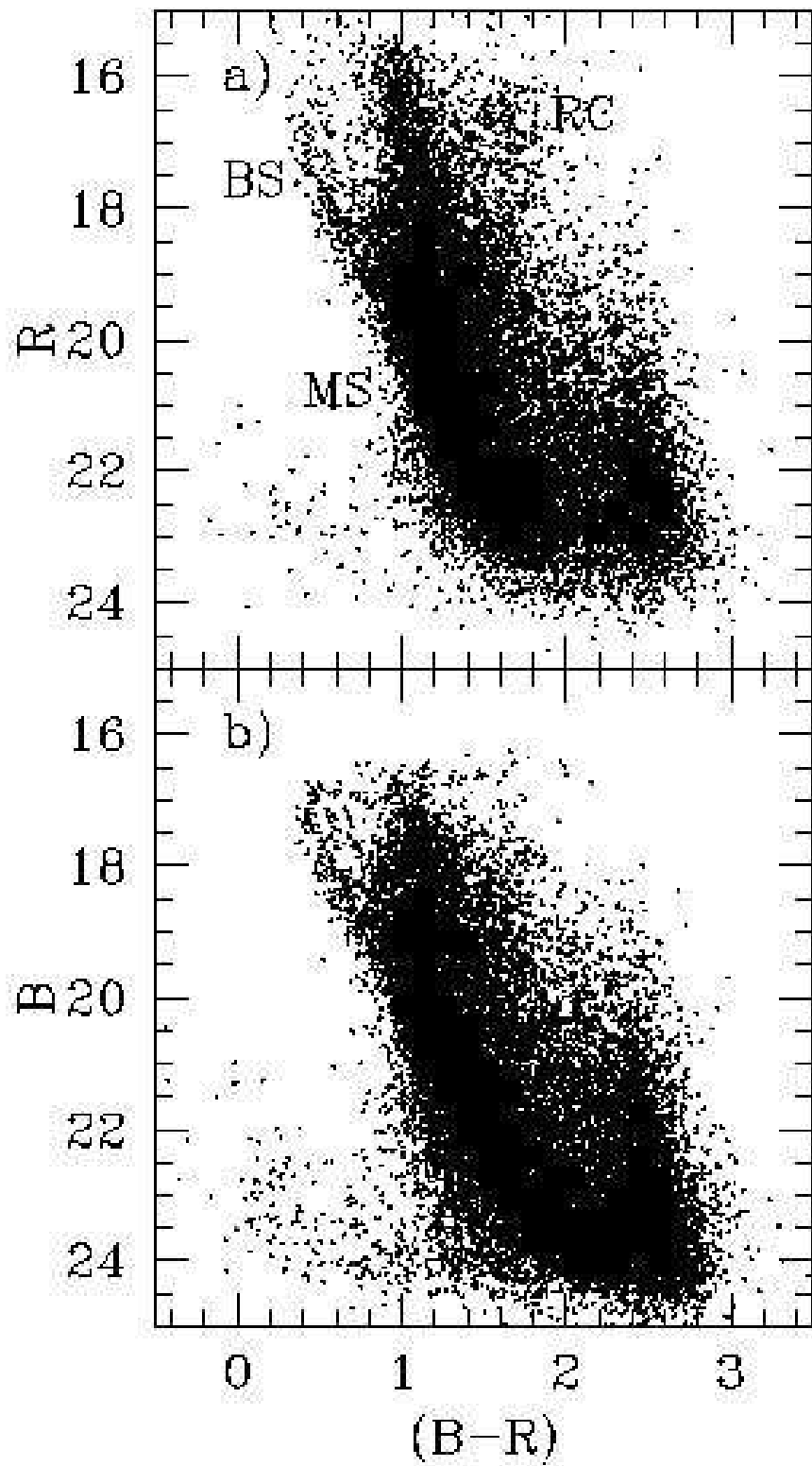
A variety of arguments suggest indeed that the CMa dwarf galaxy is currently the best candidate origin for the Monoceros stream because the dwarf appears to be un-

dergoing a tidal disruption process. Indeed, the location of the CMa dwarf, as well as its kinematical characteristics, are fairly similar to the progenitor model of the Monoceros tidal stream obtained by Peñarrubia et al. (2004). However, Martin et al. (2004b) measure proper motions for a sample of stars thought to belong to CMa dwarf that lead to a co-planar motion of the main system, whereas the Monoceros stream progenitor should follow an orbit with $i = 25 \pm 5^\circ$ with respect to the Galaxy disc in order to reproduce the vertical distribution of debris (see Peñarrubia et al. 2004). In addition, the distribution of radial velocities of M-giant stars in the centre of CMa appears to be bimodal, whereas one would expect a unique peak taking in account the surface density of CMa is several order of magnitude larger than that expected for a tidal stream (see Peñarrubia et al. 2004 for a discussion of this issue). Therefore, better constraints on the orbit of this satellite are of crucial importance for identifying it as the progenitor of the Monoceros stream.

We thank Annie Robin for her useful comments on the use of her Milky Way model www interface. DMD devotes this work to the memory of his grandfather Manuel Delgado-Membrives.

REFERENCES

Aparicio, A., Carrera, R., Martínez-Delgado, D. 2001, AJ, 122, 2524
 Bellazzini, M., Ibata, R., Monaco, L., Martin, N., Irwin, M. J., Lewis, G. F. 2004, MNRAS, in press (astro-ph/0311119)
 Binney, J., Tremaine, S., Galactic Dynamics, Princeton University Press, Princeton, New Jersey
 Butler, D. J., Martínez-Delgado, D., Brandner, W., 2004, AJ, 127, 1472
 Cardelli, J. A., Clayton, G. C., Mathis, J. S., 1989, ApJ, 345, 245
 Carrera, R., Aparicio, A., Martínez-Delgado, D., Alonso-García, J. 2002, AJ, 123, 3199
 Irwin, M. & Hatzidimitriou, D. 1995, MNRAS, 317, 831
 Navarro, J. F. 2004, in *Penetrating Bars through Marks of Cosmic Dust*, in press (astro-ph/0405947)
 Majewski S. R. 2004, in *Satellites and Tidal Streams*, Prada, Martínez-Delgado & Mahoney eds., San Francisco, ASP, ASP Conference Series vol. 327, in press.
 Martin, N. F., Ibata, R. A., Bellazzini, M., Irwin, M. J., Lewis, G. F., Dehnen, W., 2004a, MNRAS, 348, 12
 Martin, N. F., Ibata, R. A., Conn, B. C., Lewis, G. F., Bellazzini, M., Irwin, M. J., McConnachie, W., 2004b, MNRAS, in press (astro-ph/0407391)
 Martínez-Delgado, D., Gómez-Flechoso, M. A., Aparicio, A., Carrera, R. 2004, ApJ, 601, 242
 Mateo, M. L., 1998, ARAA, 36, 435
 Momany, Y., Zaggia, S. R., Bonifacio, P., Piotto, G., De Anfeli, F., Bedin, L. R., Carraro, G. 2004, A&A, 421, L29
 Newberg, H. J. et al. 2002, ApJ, 596, L191
 Pasqually, A., Larsen, S., Ferreras, I., Gnedin, O. Y., Malhotra, S., Rhoads, J. E., Pirzkal, N., Walsh, J. R. 2004, AJ, in press (astro-ph/0403338)
 Peñarrubia, J., Martínez-Delgado, D., Rix, H.-W., Gómez-Flechoso, M. A., Munn, J., Newberg, H. J., Bell, E. F., Yanny, B., Zucker, D., Grebel, E. K. 2004, ApJ, submitted (astro-ph/0410448)
 Pietrinferni, A., Cassisi, S., Salaris, M., Castelli, F., 2004, ApJ, in press, (astro-ph/0405193)
 Robin, A. C., Reyle, S., Derriere, S., Picaud, S. 2003, A&A, 409, 523
 Schlegel D. J., Finkbeiner, D. P., Davis, M., 1998, ApJ, 500, 525 (SFD98)
 Stetson, P. B. 1994, PASP, 106, 205
 Yanny, B. et al. 2003, ApJ, 588, 824



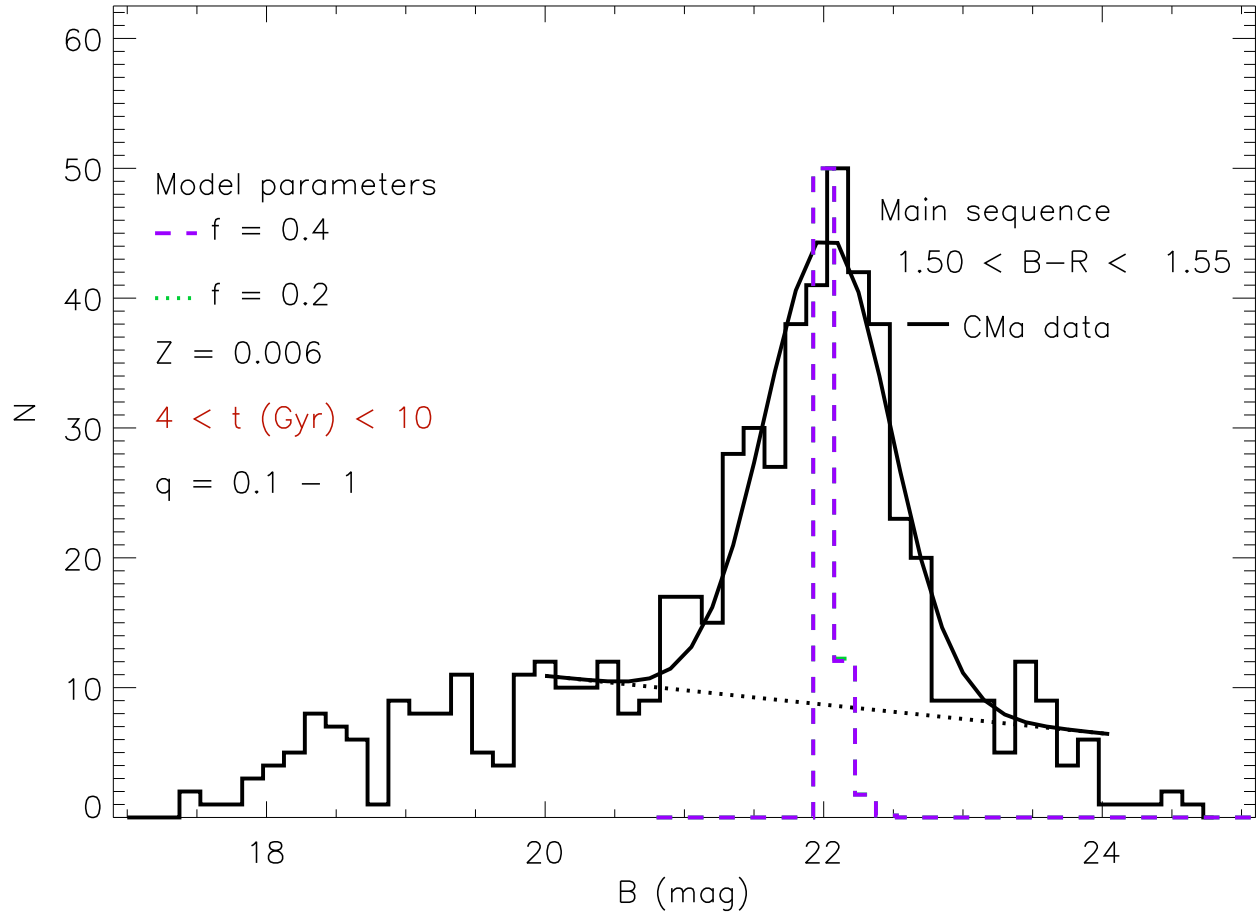


FIG. 2.— B-band histogram derived for the B-R range 1.50-1.55 mag in the long exposure data. The overlaid model data is for a binary fraction of 0.2 and 0.4 with a flat probability distribution of mass ratios between 0.1 and 1. The distribution for each binary fraction has been smoothed to mimic the effect of photometry errors, and they are indistinguishable. See the text for further details.

TABLE 1

BUDGET USED TO DETERMINE THE THICKNESS OF THE CMA MS AND AN MS MODEL WITH Z=0.006 AND AGE OF 4 TO 10 GYR

Measured main sequence thickness	
$2 \times \sigma_{MS, real, CMA, CMD}$ (mag)	0.90 ± 0.11
Model main sequence thickness ^a	
$\sigma_{B, MS, int}$ (mag) ; q=0.1 to 1; f=0.2 (or 0.4)	0.22
Random errors	
$\sigma_{B, MS, plus, phot, errors}$ (mag)	0.17^b
$\sigma_{diff, reddening, B^c}$ (mag)	0.12
Systematic error: distance (kpc)	0.3

^aZ=0.006; 4-10 Gyr; f=0.2, q=0.1-1.^bFrom artificial star tests, based on a single age population, and determined at B \sim 22.1 mag and B-R = 1.5 to 1.55 mag.^cAdopted the Cardelli, Mathis & Clayton (1989) reddening law and took the rms diff. reddening in the B-V index to be 0.029 magTABLE 2
RELEVANT PROPERTIES OF THE CMA FIELD.

I (deg)	240.15
b (deg)	-08.07
E(B-V) (mag)	0.213 ± 0.029^a
d (kpc)	5.3 ± 0.2^b to 8.1 ± 0.4^c
Δd (kpc)	$1.60 \pm 0.20 \pm 0.10^d$
$r_{1/2}/FWHM$ (kpc)	$0.93 \pm 0.25 \pm 0.36$
$\mu_{V,0}^e$ (mag arcsec $^{-2}$)	$\geq 24.1 \pm 1.8^c$
M_V^e (mag)	-13.8 ± 1.8
$\log(I_V/I_{V,\odot})^f$	$< 7.4 \pm 0.7$

^aIn the WFI field of view^bModel used: Z=0.0004, 15 Gyr, f=0.2, q=0.1-1^cModel used: Z=0.006, 4-10 Gyr, f=0.2, q=0.1-1^d $2 \times \sigma$ line-of-sight size^eModel used: Z=0.006, 2.5-15 Gyr. Adopted an exponential density profie for CMa (taken from Martin *et al.* 2004).^f Logarithm of the estimated V-band intensity of CMa, $\log(I_V) = 0.4(4.83 - M_V)$